Molecular Solar Cells

Panchromatic Response in Solid-State Dye-Sensitized Solar Cells Containing Phosphorescent Energy Relay Dyes**

Jun-Ho Yum, Brian E. Hardin, Soo-Jin Moon, Etienne Baranoff, Frank Nüesch, Michael D. McGehee, Michael Grätzel, and Mohammad K. Nazeeruddin**

Dye-sensitized solar cells (DSCs) based on nanocrystalline semiconductors have been intensively studied because of their potential low cost, easy processing, and high performance.[1] Besides broadening light absorption into the near-infrared domain, enhancing the open-circuit potential is a key pathway to further increase the power-conversion efficiency. In a typical liquid-electrolyte cell the maximum open-circuit potential is around 800 mV, which is significantly less than those of solid-state dye-sensitized solar cells (SSDSCs) composed of organic hole-transporting materials (HTMs).[2] By minimizing the energy difference between the HOMO of the sensitizing dye and the work function of the organic hole conductor, it is possible to develop DSCs with higher power-conversion efficiency. Recently, we demonstrated SSDSCs with open-circuit voltage greater than 1000 mV with the promise of high power-conversion efficiency.[3] However, SSDSCs suffer from significantly higher recombination rates and are limited to optimized thicknesses of about 2 μm (versus 10 μm for liquid DSCs),[4] which limits light absorption. Hence, the primary challenge with SSDSCs is to absorb all the light inside a relatively thin film.

Schemes developed to increase light absorption in liquid DSCs include co-sensitization[5] and the use of intramolecular energy transfer between energy-donor molecules covalently attached to the sensitizing dye.[6] Although these architectures can broaden light absorption, they require that the dyes attach to the titania surface, which does not allow for increased dye loading. We recently demonstrated a new DSC architecture in which highly luminescent energy-relay dyes (ERDs) placed inside the electrolyte absorb higher energy photons and transfer their energy to the sensitizing dye by Förster resonant energy transfer (FRET).[7] A DSC architecture with an ERD allows separation of light-absorption and charge-transfer processes. Herein, an ERD was introduced at high concentrations inside the HTM to increase the light harvesting yield of SSDSCs, as shown in Figure 1 (see Supporting Information, Scheme S1 for energy diagram).
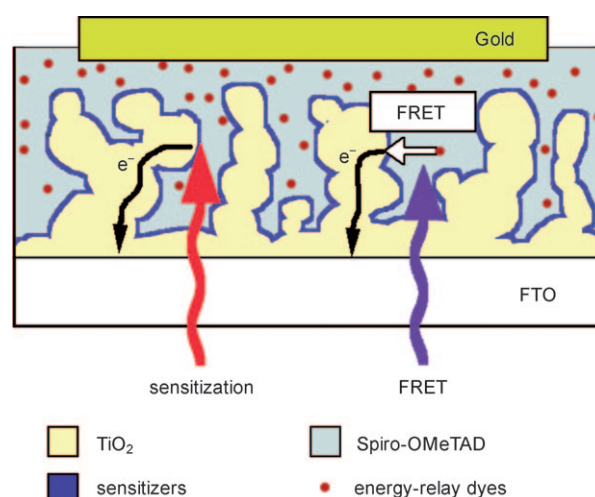

Figure 1. Operating mechanism of an SSDSC. Absorption of lower energy (red) photons by the sensitizing dye (SQ1) transfers an electron into the TiO$_2$ and a hole into the electrolyte. Higher energy (blue) photons are absorbed by the energy-relay dye (N877) and transferred by FRET to the sensitizing dye. Figure is not drawn to scale.

The ERDs used in SSDSCs should be soluble in polar solvents (e.g., chlorobenzene), mix well, and not undergo photoreactions with the HTM. In SSDSCs, hole injection from the sensitizing dye to the Spiro-OMeTAD hole transporter occurs within 1 ps to 4 ns (Spiro-OMeTAD: 2,2′,7,7′-tetrakis-(*N*,*N*-di-*p*-methoxyphenylamine)9,9′-spirobifluorene).[8] We used a highly phosphorescent phenanthroline ruthenium(II) sensitizer (hereafter denoted N877) as energy-

[*] Dr. J.-H. Yum, S.-J. Moon, Dr. E. Baranoff, Prof. M. Grätzel,
Prof. M. K. Nazeeruddin
LPI, Institut des Sciences et Ingénierie Chimiques
Faculté des Sciences de Base, École Polytechnique Fédérale de
Lausanne
1015 Lausanne (Switzerland)
Fax: (+41) 21-693-4111
E-mail: michael.graetzel@epfl.ch
            mdkhaja.nazeeruddin@epfl.ch

B. E. Hardin, Prof. M. D. McGehee
Department of Material Science and Engineering
Stanford University
Stanford, California 94305-4045 (USA)

Dr. F. Nüesch
Laboratory for Functional Polymers, Empa
Swiss Federal Laboratories for Materials Testing and Research
Überlandstrasse 129, 8600 Dübendorf (Switzerland)

Prof. M. K. Nazeeruddin
WCU, Department of Chemistry, Korea University
208 Seochang, Chochiwon, Chung-nam 339-700 (Korea)

relay dye, and an efficient near-infrared sensitizer (SQ1)[9] (for molecular structures, see Figure S1 of the Supporting Information) in SSDSCs based on Spiro-OMeTAD. The ERDs absorb higher energy photons and transfer the energy to SQ1 without contribution of direct charge injection to TiO$_2$, as shown in Scheme S1 (Supporting Information). To the best of our knowledge, this is the first time ERDs have been incorporated in SSDSCs.

Förster resonant energy transfer involves dipole–dipole coupling of the ERD and sensitizing dye through the electric dipole field.[10] A good measure of the field strength is the FRET radius R_o, which is defined as the distance at which the probability of FRET between donor (i.e., N877) and acceptor (i.e., SQ1) is 50%. The R_o value is dependent on the photoluminescence (PL) efficiency of the ERD and the overlap between ERD emission (phosphorescence) and the molar extinction coefficient of the sensitizing dye (see Supporting Information). The UV/Vis absorption spectrum (Figure 2) of SQ1 in ethanol shows a maximum at 636 nm
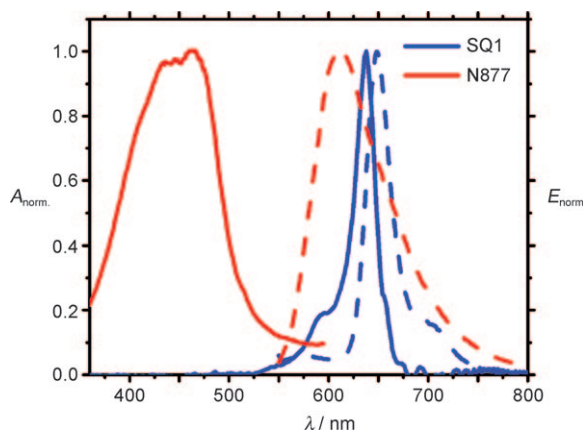

Figure 2. Normalized UV/Vis absorption (solid line)/emission (dashed line) spectra of SQ1 (blue) and N877 (red) in ethanol.

with high molar extinction coefficient ($\varepsilon = 158\,500\,\mathrm{M}^{-1}\mathrm{cm}^{-1}$) due to strong π–π^* charge-transfer (CT) transitions.[9] The absorption maximum of N877 occurs at 460 nm ($29\,000\,\mathrm{M}^{-1}\mathrm{cm}^{-1}$), and the emission maximum at 612 nm. As shown in Figure 2, the emission range of N877 matches well with the absorption range of SQ1, and the phosphorescence quantum yield of N877 in solution is 37% at room temperature[11] and 68% at 77 K.[12] The calculated R_o is about 5.0 nm based on 37% quantum yield for the N877/SQ1 system and was experimentally verified by time-resolved PL spectroscopy (Figures S2 and S3 in the Supporting Information). For a quantum yield of 68% the Förster radius increases to 6.3 nm.

One of the biggest challenges in using ERDs in SSDSCs that must be overcome is quenching of the excited ERD by the hole conductor. High quenching rates compete with FRET and reduce the excitation transfer efficiency.[7] To determine the degree of PL quenching, the photoluminescence of N877 inside Spiro-OMeTAD was compared to that of N877 in an inert polystyrene matrix. Films were spun-cast at 1000 rpm onto a glass substrate from a solution of 1.5 wt%

N877 in 27 mg mL^{-1} of polystyrene or Spiro-OMeTAD in chloroform inside a glove box. The sensitizer N877 tends to form aggregates in chlorobenzene, but completely dissolves in chloroform. Figure S5 (Supporting Information) compares the photoluminescence of N877/Spiro-OMeTAD and N877/polystyrene films, corrected for differences in absorption. The peak PL is 69 times lower in Spiro-OMeTAD than in polystyrene. Cyclic voltammetry indicates that the first oxidation potential of Spiro-OMeTAD is about 0.81 V versus the normal hydrogen electrode,[13] while the potential of N877 HOMO is about 1.46 V.[14] There are several possible reasons for the relatively ineffective quenching, which is assigned to hole injection from the excited sensitizer into Spiro-OMeTAD. The N877 sensitizer does not contain NCS ligands, which are typically introduced into sensitizing dyes and are known to increase hole transfer,[15] and the large difference between the energy levels may retard charge injection from Spiro-OMeTAD (see Scheme S1, Supporting Information). A full description of the relationship between ERD HOMO level and charge injection is beyond the scope of this paper and will be discussed in a future study.

Figure 3 shows the incident monochromatic photon-to-current conversion efficiency (IPCE) of SSDSCs sensitized by SQ1 with and without N877. At the peak absorption wave-
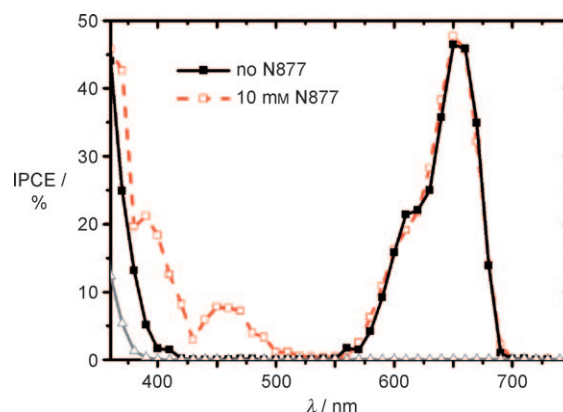

Figure 3. IPCE spectrum of SQ1 SSDSCs with and without N877 ERD. Gray line: Spiro-OMeTAD + N877. Black line: SQ1 + Spiro-OMeTAD. Red line: SQ1 + N877 + Spiro-OMeTAD.

length, IPCE exceeds 47% in SQ1-sensitized solid-state solar cells, but only 76% of the light is absorbed, giving an internal quantum efficiency (IQE) of 62%. When 10 mM of N877 is added, the IPCE increases to 8% at 460 nm and 21% at 400 nm, resulting in 30% increase in current density and 29% increase in power-conversion efficiency (Table 1). The observed increase in photogenerated current could be caused by direct injection from N877 to TiO$_2$. To see whether this process occurs, we made an SSDSC containing no sensitizer while keeping all other conditions unchanged. The data clearly show no injection of electrons in the visible region between 400 and 500 nm (Figure 3, gray line) and corroborate the hypothesis that the new IPCE from 400 to 530 nm is caused by energy transfer from N877 to SQ1.

Table 1: *J–V* characteristics of SQ1 SSDSCs without and with N877.

[N877] [mM]	J_{sc} [mA cm^{-2}]	V_{oc} [mV]	Fill factor (FF)	η [%][a]
0[b]	2.98	807	0.58	1.40
10[c]	3.87	786	0.59	1.80

[a] Overall efficiency η is derived from $J_{sc} \times V_{oc} \times$ FF/light intensity. [b] Active area: 0.35 cm^2. [c] Active area: 0.36 cm^2.

The excitation transfer efficiency (ETE) is the fraction of excited unattached chromophores (i.e., N877 dyes) that transfer their energy to the sensitizing dye (i.e., SQ1).[7] The ETE [Eq. (1)] can be determined from the ERD light absorption, device IQE, and change in IPCE. Figure 3 shows a ΔIPCE of 8% and IQE of 62%. For a film thickness of 2 μm and porosity of 0.60, the measured $\eta_{abs,donor}$ is 41% and an ETE of 32% can be estimated.

$$\text{ETE} = \frac{\Delta\text{IPCE}}{\text{IQE} \cdot \eta_{abs,donor}} \qquad (1)$$

In conclusion, we have demonstrated Förster energy transfer in solid-state dye-sensitized solar cells between a phosphorescent ruthenium complex solvated in the solid organic hole conductor Spiro-OMeTAD and squaraine dyes grafted on the oxide surface. By incorporating ERD into the SSDSC it is possible to greatly increase dye loading. By using a combination of red-light sensitizing dyes with high molar extinction coefficient and ERDs that absorb in the visible region it is possible to significantly increase light-harvesting yields in thin-film DSCs. The ERD in Spiro-OMeTAD increased the efficiency of the optimized SQ1 SSDSCs by 29% in terms of power-conversion efficiency. The low PL quenching is an important parameter in this system that leads to retarded direct charge injection before FRET transfer. This device architecture has the potential to improve DSC efficiency by choosing sensitizing dyes with higher internal quantum efficiencies and energy-relay dyes with higher phosphorescent quantum yields that are minimally quenched by Spiro-OMeTAD.

Experimental Section

Synthesis of SQ1: The detailed procedure for synthesis of SQ1 was described in our previous work.[9]

Synthesis of tris(4,7-diphenyl-1,10-phenanthroline)ruthenium(II) chloride, [Ru(dpp)$_3$]Cl$_2$ (N877, see synthetic route in Figure S6, Supporting Information): The ligand dpp and [{RuCl$_2$(*p*-cymene)}$_2$] were obtained from Aldrich and used as received. All reagents and solvents purchased were of reagent grade (puris) from Fluka and were used without further purification. The complex was synthesized in a commercial microwave oven (CEM, Discover) in a septum-sealed 10 mL glass tube. In a typical reaction [{RuCl$_2$(*p*-cymene)}$_2$] (0.0612 g, 0.1 mmol) and dpp (0.233 g, 0.7 mmol) were placed in a 10 mL glass tube and DMF (2 mL) was added. A magnetic stir bar (5 × 2 mm) was introduced into the reaction tube. Then the tube was sealed with a septum (CEM) and inserted into a microwave oven. The reaction mixture was heated to reflux at 220°C for 5 min under stirring with a 300 W microwave source. After cooling the reaction tube, the complex was precipitated with diethyl ether (ca. 20 mL). The isolated bright red-orange solid was dissolved in dichloromethane (ca. 2 mL) and again precipitated by adding diethyl ether (ca. 20 mL) to give 0.207 g (89%). Elemental analysis (%): calcd for [Ru(dpp)$_3$]Cl$_2$·6 H$_2$O$_6$: C$_{72}$H$_{60}$Cl$_2$N$_6$O$_6$Ru: C 67.71, H 4.73, N 6.58; found: C 66.78, H 4.60, N 6.56. C/N ratio calcd: 12; found: 11.873.

Absorption and photoluminescence measurement: UV/Vis absorption spectra were measured on a Cary 5 spectrophotometer, and fluorescence spectra on a Spex Fluorolog 112 spectrofluorimeter. Samples were contained in quartz cells with 1 cm path length. Time-resolved PL measurements were performed by using a time-correlated single-photon counting (TCSPC) system from PicoQuant. Solutions were excited with a pulsed laser diode (model LDH 485: 481 nm, 70 ps FWHM, 5 MHz) and PL detected with a single-photon avalanche diode (PDM 100CT SPAD) attached to a monochromator and processed by a PicoHarp 300 correlating system.

Solar cell fabrication: For solid-state solar cells, fluorine-doped SnO$_2$ glass (15 Ω/square, Pilkington) substrates were cleaned first with Helmanex solution and rinsed with acetone and then ethanol. Next, a ca. 100 nm compact layer of TiO$_2$ was deposited by spray pyrolysis.[16] A porous layer of 30 nm TiO$_2$ particles (ca. 2 μm thick) was coated by the doctor-blade technique, followed by sintering at 500°C under an oxygen flow. After cooling, the thin TiO$_2$ films were impregnated in a 0.02 M aqueous TiCl$_4$ solution for 15 h, and then rinsed with deionized water. The TiCl$_4$-treated TiO$_2$ films were annealed at 450°C for 30 min and then cooled to about 80°C before plunging into the dye solution for 3 h. After soaking in dye solution, the substrates were rinsed in acetonitrile, and then a solution of Spiro-OMeTAD (180 mg mL^{-1} in chlorobenzene) with *tert*-butylpyridine (17 μL mL^{-1}) and Li[CF$_3$SO$_2$]$_2$N (19.5 mM) as additives was spin-coated at 2000 rpm on top of the TiO$_2$ film.[2f,g] For energy-transfer studies, 10 mM of N877 in the Spiro-OMeTAD solution was spin-coated. Finally, a 50 nm gold layer was evaporated onto the top of the Spiro-OMeTAD.

Solar-cell characterization: For photovoltaic measurements on the DSCs, the irradiation source was a 450 W xenon light source (Osram XBO 450, USA) with a filter (Schott 113), the power of which was regulated to the AM 1.5G solar standard by using a reference Si photodiode equipped with a color-matched filter (KG-3, Schott) to reduce the mismatch in the region of 350–750 nm between the simulated light and AM 1.5G to less than 4%. The measurement delay time of photo-*J–V* characteristics of DSCs was fixed to 40 and 100 ms for liquid solar cells and solid solar cells, respectively. The incident photon-to-current conversion efficiency (IPCE) was plotted as a function of excitation wavelength by using the incident light from a 300 W xenon lamp (ILC Technology, USA), which was focused through a Gemini-180 double monochromator (Jobin Yvon Ltd.).

[1] a) B. O'Regan, M. Grätzel, *Nature* **1991**, *353*, 737; b) M. A. Green, K. Emery, Y. Hisikawa, W. Warta, *Prog. Photovoltaics* **2007**, *15*, 425.

[2] a) K. Tennakone, G. R. R. A. Kumara, A. R. Kumarasinghe, K. G. U. Wijayantha, P. M. Sirimanne, *Semicond. Sci. Technol.* **1995**, *10*, 1689; b) J. Hagen, W. Schaffrath, P. Otschik, R. Fink, A. Bacher, H. W. Schmidt, D. Haarer, *Synth. Met.* **1997**, *89*, 215; c) U. Bach, D. Lupo, P. Comte, J. E. Moser, F. Weissortel, J. Salbeck, H. Spreitzer, M. Grätzel, *Nature* **1998**, *395*, 583; d) B. O'Regan, F. Lenzmann, R. Muis, J. Wienke, *Chem. Mater.* **2002**, *14*, 5023; e) H. J. Snaith, A. J. Moule, C. Klein, K. Meerholz, R. H. Friend, M. Grätzel, *Nano Lett.* **2007**, *7*, 3372.

Communications

[3] P. Chen, J. H. Yum, F. De Angelis, E. Mosconi, S. Fantacci, S. J. Moon, R. H. Baker, J. Ko, M. K. Nazeeruddin, M. Grätzel, *Nano Lett.* **2009**, *9*, 2487.

[4] L. Schmidt-Mende, S. M. Zakeeruddin, M. Grätzel, *Appl. Phys. Lett.* **2005**, *86*, 013504.

[5] a) A. Ehret, L. Stuhl, M. T. Spitler, *J. Phys. Chem. B* **2001**, *105*, 9960; b) K. Sayama, S. Tsukagoshi, T. Mori, K. Hara, Y. Ohga, A. Shinpou, Y. Abe, S. Suga, H. Arakawa, *Sol. Energy Mater. Sol. Cells* **2003**, *80*, 47; c) Y. S. Chen, Z. H. Zeng, C. Li, W. B. Wang, X. S. Wang, B. W. Zhang, *New J. Chem.* **2005**, *29*, 773; d) J. J. Cid, J. H. Yum, S. R. Jang, M. K. Nazeeruddin, E. M. Ferrero, E. Palomares, J. Ko, M. Grätzel, T. Torres, *Angew. Chem.* **2007**, *119*, 8510; *Angew. Chem. Int. Ed.* **2007**, *46*, 8358; e) J. H. Yum, S. R. Jang, P. Walter, T. Geiger, F. Nüesch, S. Kim, J. Ko, M. Grätzel, M. K. Nazeeruddin, *Chem. Commun.* **2007**, 4680.

[6] a) R. Amadelli, R. Argazzi, C. A. Bignozzi, F. Scandola, *J. Am. Chem. Soc.* **1990**, *112*, 7099; b) C. Siegers, J. Hohl-Ebinger, B. Zimmerrnann, U. Wurfel, R. Mulhaupt, A. Hinsch, R. Haag, *ChemPhysChem* **2007**, *8*, 1548; c) H. N. Tian, X. C. Yang, J. X. Pan, R. K. Chen, M. Liu, Q. Y. Zhang, A. Hagfeldt, L. C. Sun, *Adv. Funct. Mater.* **2008**, *18*, 3461; d) C. Siegers, B. Olah, U. Wurfel, J. Hohl-Ebinger, A. Hinsch, R. Haag, *Sol. Energy Mater. Sol. Cells* **2009**, *93*, 552.

[7] B. E. Hardin, E. T. Hoke, P. B. Armstrong, J. H. Yum, T. Torres, J. M. J. Fréchet, M. K. Nazeeruddin, M. Grätzel, M. D. Mcgehee, *Nat. Photonics* **2009**, *3*, 406.

[8] U. Bach, Y. Tachibana, J.-E. Moser, S. A. Haque, J. R. Durrant, M. Grätzel, D. R. Klug, *J. Am. Chem. Soc.* **1999**, *121*, 7445.

[9] J. H. Yum, P. Walter, S. Huber, D. Rentsch, T. Geiger, F. Nüesch, F. De Angelis, M. Grätzel, M. K. Nazeeruddin, *J. Am. Chem. Soc.* **2007**, *129*, 10320.

[10] T. Förster, *Ann. Phys.* **1948**, *2*, 55.

[11] M. J. Cook, A. J. Thomson, *Chem. Br.* **1984**, *20*, 914.

[12] R. J. Watts, G. A. Crosby, *J. Am. Chem. Soc.* **1972**, *94*, 2606.

[13] U. B. Cappel, E. A. Gibson, A. Hagfeldt, G. Boschloo, *J. Phys. Chem. C* **2009**, *113*, 6275.

[14] C. T. Lin, W. Bottcher, M. Chou, C. Creutz, N. Sutin, *J. Am. Chem. Soc.* **1976**, *98*, 6536.

[15] M. K. Nazeeruddin, Q. Wang, L. Cevey, V. Aranyos, P. Liska, E. Figgemeier, C. Klein, N. Hirata, S. Koops, S. A. Haque, J. R. Durrant, A. Hagfeldt, A. B. P. Lever, M. Grätzel, *Inorg. Chem.* **2006**, *45*, 787.

[16] L. Kavan, M. Grätzel, *Electrochim. Acta* **1995**, *40*, 643.